-Supplementary Information

Boosting Electrochemical Nitrogen Reduction to Ammonia with High Efficiency using LiNb$_3$O$_8$ Electrocatalyst in Neutral Media

Qi Wang, Shuhui Fan, Leran Liu, Xiaojiang Wen, Yun Wu, Rui Yao, Qiang Zhao,

Jinping Li, Guang Liu*

1. Determination of NH_4^+

The concentration of NH_4^+ was quantitatively determined by Indophenol blue colorimetry.

Preparation of chromogenic agent： 2 mL of 5wt% sodium citrate dehydrate-salicylic acid solution, 1 mL of sodium hypochlorite solution (0.05M), 0.2 mL of sodium nitroferricyanide dihydrate aqueous solution (1 wt%).

After 2 h of electrolysis, 2.0 mL of cathode electrolyte was mixed and slightly shaken with the above chromogen solution added in turn. After the reaction of mixed solution for 2 h, the curves were scanned in an ultraviolet spectrophotometer with the non-electrolytic electrolyte as blank contrast. The concentration of NH_4^+ can be obtained by substituting the absorbance at the wavelength of 655 nm into the standard working curve of NH_4^+.

Standard working curve of NH_4^+: The linear relationship between the absorbance and NH_4^+ concentration can be obtained by measuring the absorbance curves corresponding to the standard ammonia solutions with different concentration gradients. The fitting curve (y =0.4437x+0.0014, R^2=0.9996) shows good linear relation of absorbance value with NH_4^+ concentration, as shown in Fig.S9. The standard curves and fitting curve in acidic and alkaline electrolytes were tested in the same way, and the results are shown in Fig.S10.

The standard curve and fitting curve of the Nessler reagent used for control are shown in Fig.S11.

2. Determination of N_2H_4

The concentration of N_2H_4 was quantitatively determined by Watt and Chrisp method.

Preparation of chromogenic agent： 2mL of P-dimethylamino-benzaldehyde solution (0.2998 g p-dimethylamino-benzaldehyde powder, 15 mL of ethanol and 1.5 mL of concentrated hydrochloric acid).

After 2 h of electrolysis, 2.0 mL of cathodic electrolyte was mixed

with 2 ml of chromogenic solution and slightly shaken. Then the mixture reacted for 20 min, the curves were scanned in an ultraviolet spectrophotometer and pure water was used as blank contrast. The concentration of N_2H_4 can be obtained by subbing the absorbance at the wavelength of 455 nm into the N_2H_4 standard working curve.

Standard working curve of N_2H_4: The linear relationship between the absorbance and N_2H_4 concentration can be obtained by measuring the absorbance curves corresponding to the standard N_2H_4 solutions with different concentration gradients. The fitting curve (y = 0.9843 x + 0.0151, R^2 = 1) shows good linear relation of absorbance value with N_2H_4 concentration, as is shown in Fig.S12.

3. Calculation of ammonia yield rate and faradaic efficiency

Ammonia yield rate （r_{NH_3}） is calculated by the formula:

$$r_{NH_3} = \frac{\left[NH_4^+\right] \times V}{t \times m_{cat}}$$

Faradaic efficiency（FE）is calculated by the formula:

$$FE = \frac{3F \times m_{NH_3}}{17 \times Q}$$

Where [NH_4^+] is the concentration of ammonia in the electrolyte ($\mu g \cdot mL^{-1}$); V represents the volume of the electrolyte(mL); t is the reduction time (h); m_{cat} is the loaded mass of catalyst on carbon paper (μg). F is the Faraday constant (96485 C/mol); Q is the amount of electricity consumed in the electrolysis process (C); m_{NH_3} is the quality of the ammonia.

4. Calculation of ECSA

The electrochemical double-layer capacitance (C_{dl}) of the materials was measured to determine their electrochemical surface area (ECSA) using the cyclic voltammetry curves (CVs) in no faradic processes between 0.5 V vs. RHE and 0.6 V vs. RHE with diverse scan rates of 10, 20, 30, 50, 70, and 90 mV/s, respectively. The plotted current

density current density differences ($\Delta j/2$) at 0.55 V vs. RHE have a linear relationship with different scan rates and its slope is twice the C_{dl}. The specific capacitance for a flat surface is generally found to be in the range of 20~60 μF cm^{-2}, and we plug in 40 μF cm^{-2} in the following calculation.

The ECSA of LNO/CP can then be calculated as following:

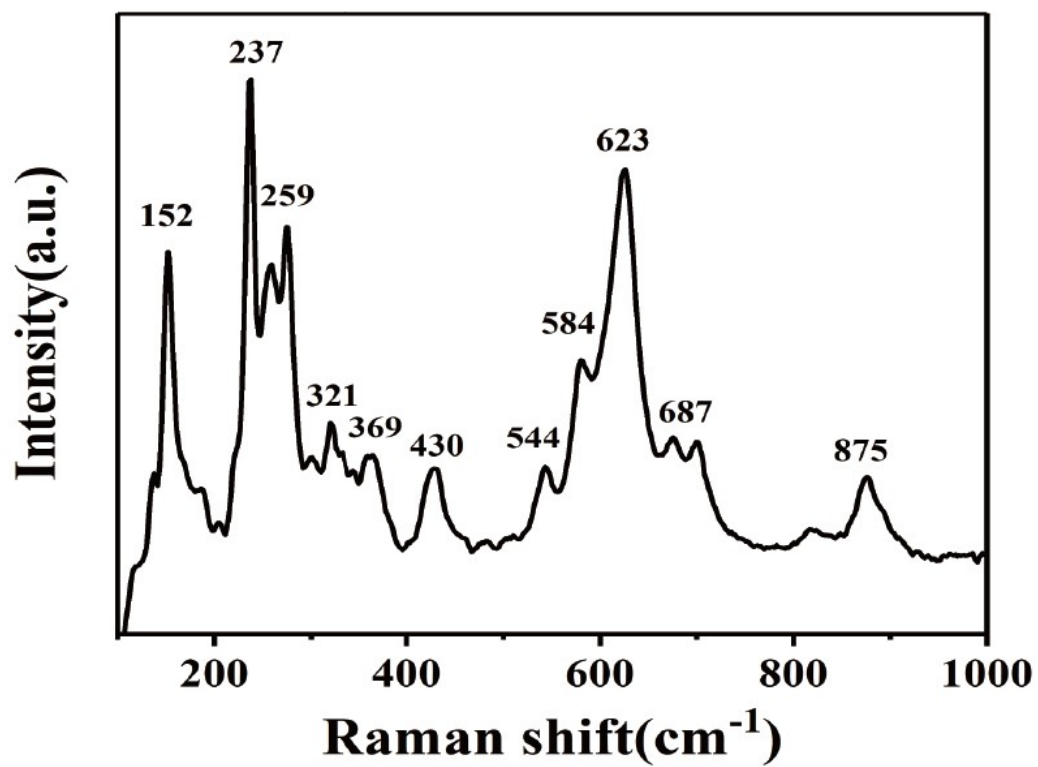$$ECSA = \frac{0.24\ mF\ cm^{-2}}{40\ \mu F cm^{-2}} = 6.0\ cm^2_{ECSA}$$

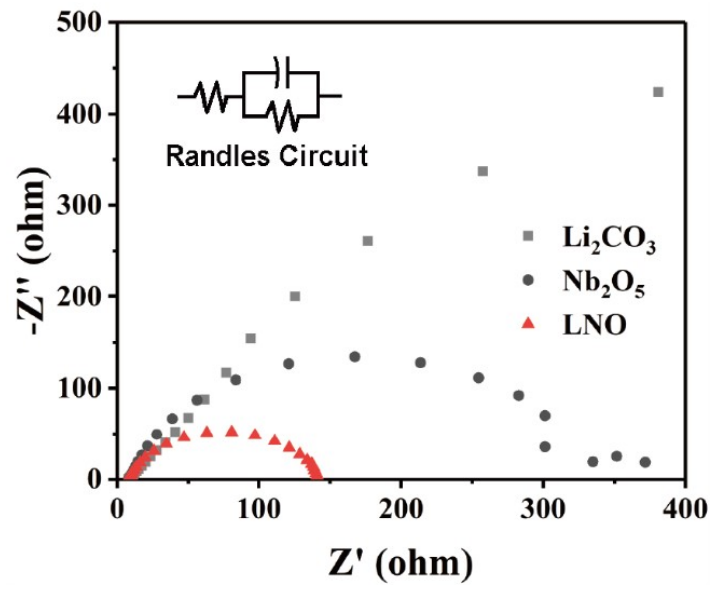Fig.S1. Raman spectrum of LNO.
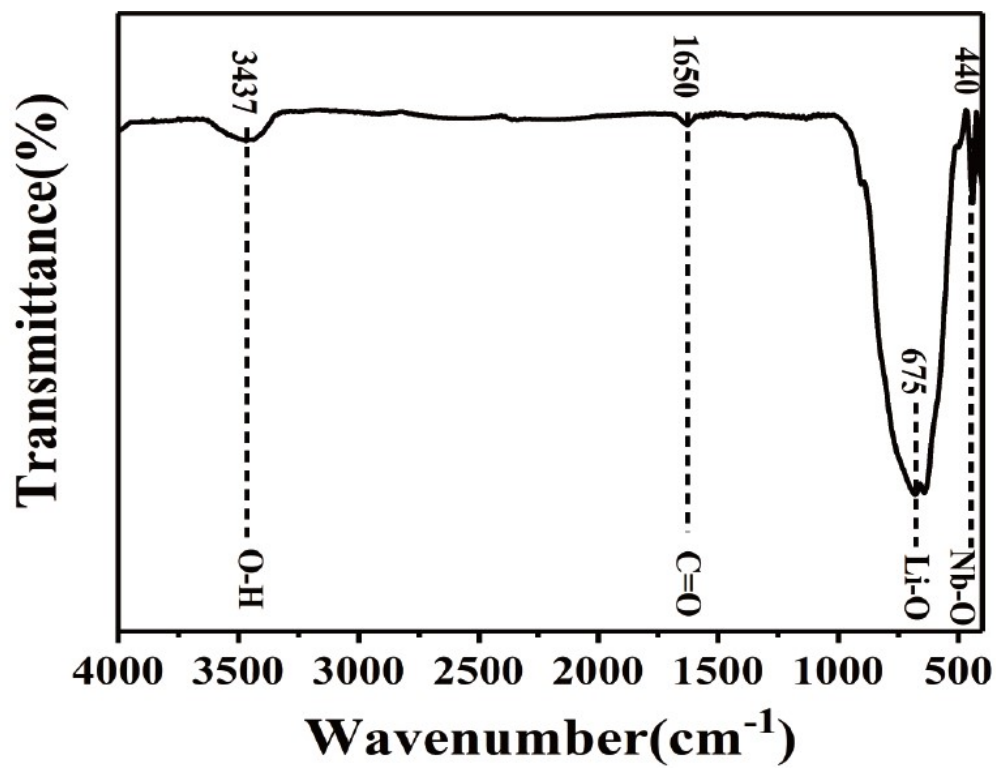
Fig.S2. FTIR spectrum of LNO.

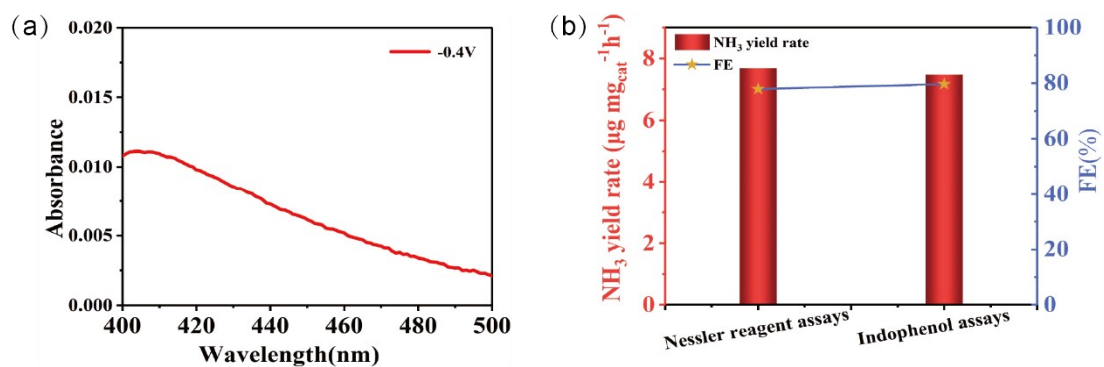Fig. S3. EIS Nyquist plots of Li_2CO_3, Nb_2O_5 and LNO.

Fig.S4. (a) UV-vis absorption spectra using Nessler reagent assays. (b) NH$_3$ yield rate and FE of LNO after NRR electrolysis using Nessler reagent assays and Indophenol assays.
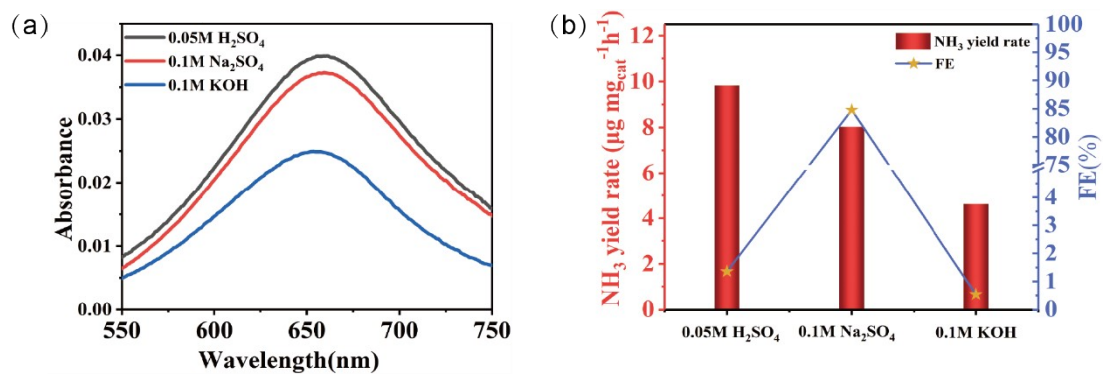
Fig.S5. (a) UV-vis absorption spectra in different electrolyte (0.05M H_2SO_4 、0.1M Na_2SO_4、 0.1M KOH). (b) NH_3 yield rate and FE of LNO after NRR electrolysis in different electrolyte.
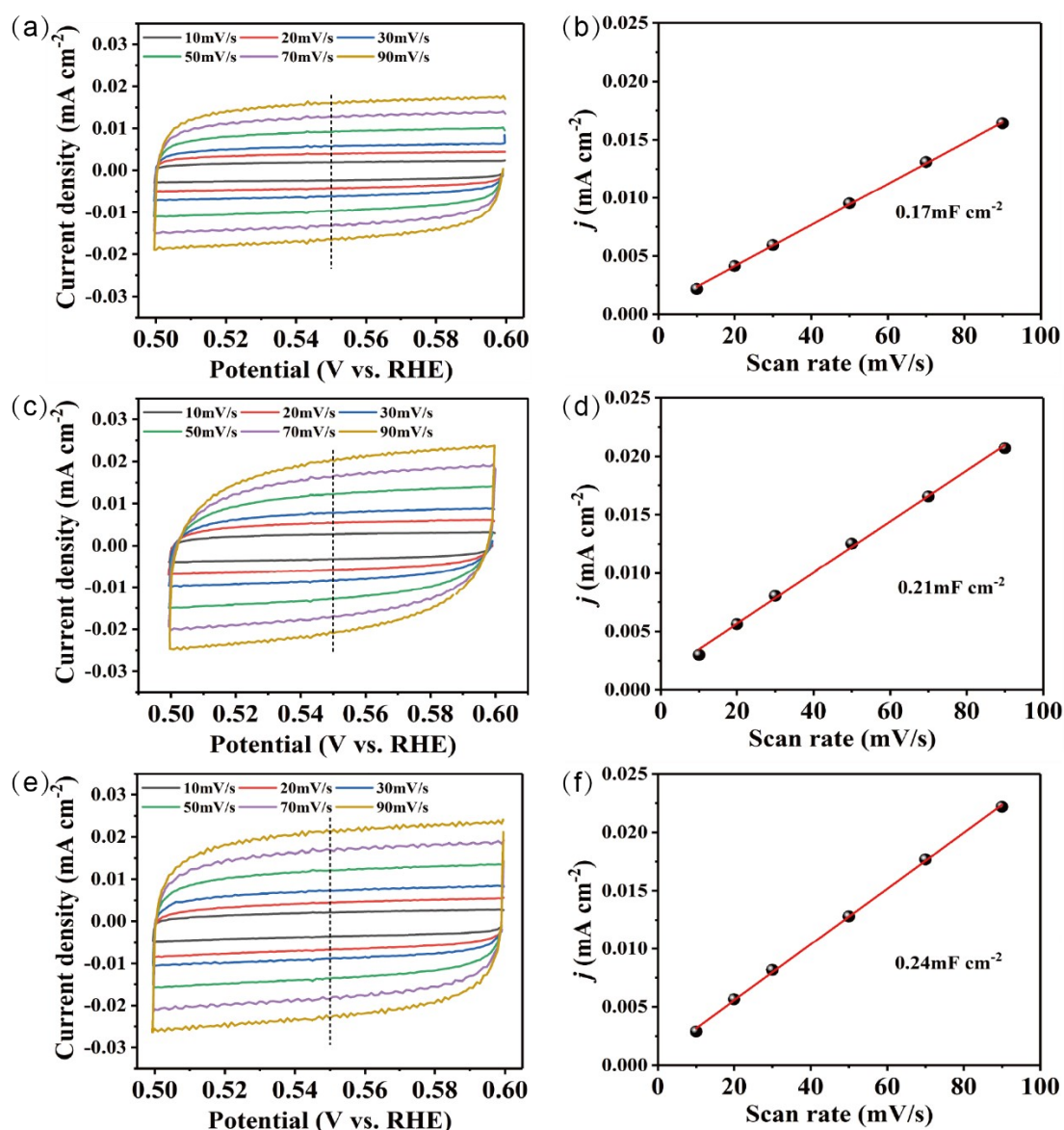
Fig.S6. (a) Cyclic voltammetry curves and (b) Plots of current density differences ($\Delta j/2$) at 0.55V with different scan rates of Nb_2O_5/CP. (c) Cyclic voltammetry curves and (d) Plots of current density differences ($\Delta j/2$) at 0.55V with different scan rates of Li_2CO_3/CP. (e) Cyclic voltammetry curves and (f) Plots of current density differences ($\Delta j/2$) at 0.55V with different scan rates of LNO/CP.
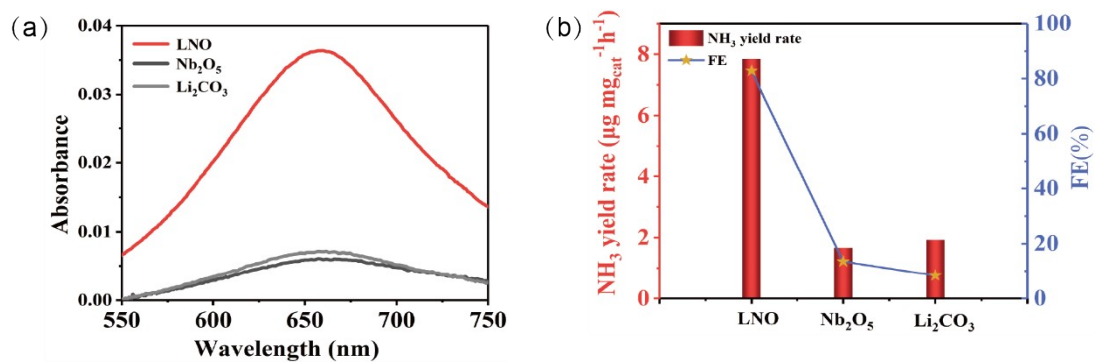
Fig.S7. (a) UV-vis absorption spectra using different catalyst (Nb_2O_5, Li_2CO_3, LNO). (b) NH_3 yield rate and FE after NRR electrolysis using different catalyst (Nb_2O_5, Li_2CO_3, LNO).
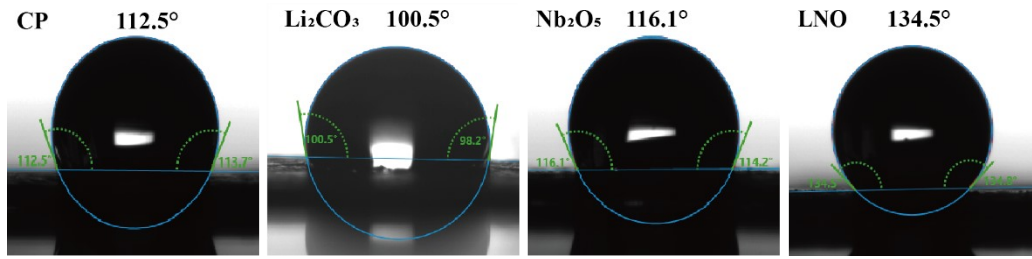
Fig.S8. Contact angles for blank CP, Li$_2$CO$_3$/CP, Nb$_2$O$_5$/CP and LNO/CP.

Fig.S9. (a) UV-vis absorption spectra of Indophenol assays with NH_3 in 0.1 M Na_2SO_4 after incubated for 2h under ambient conditions. (b) Calibration curve used for calculation of NH_3 concentration.
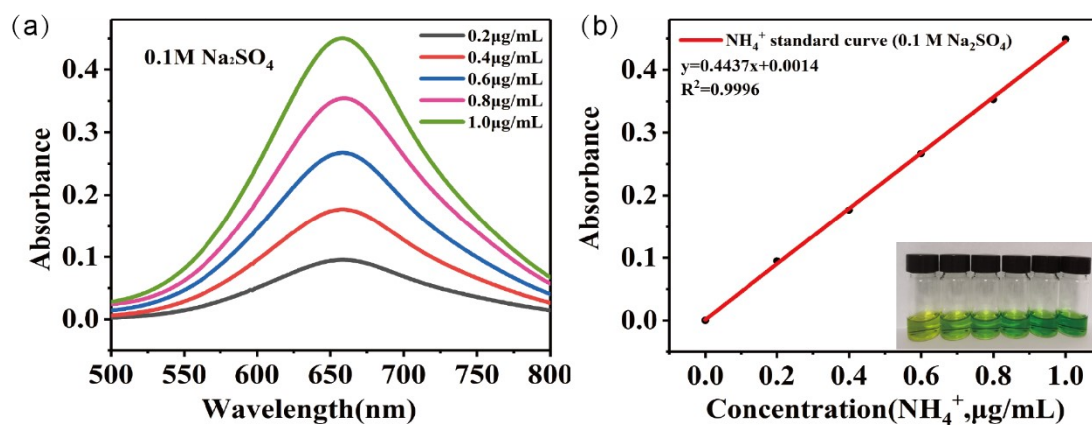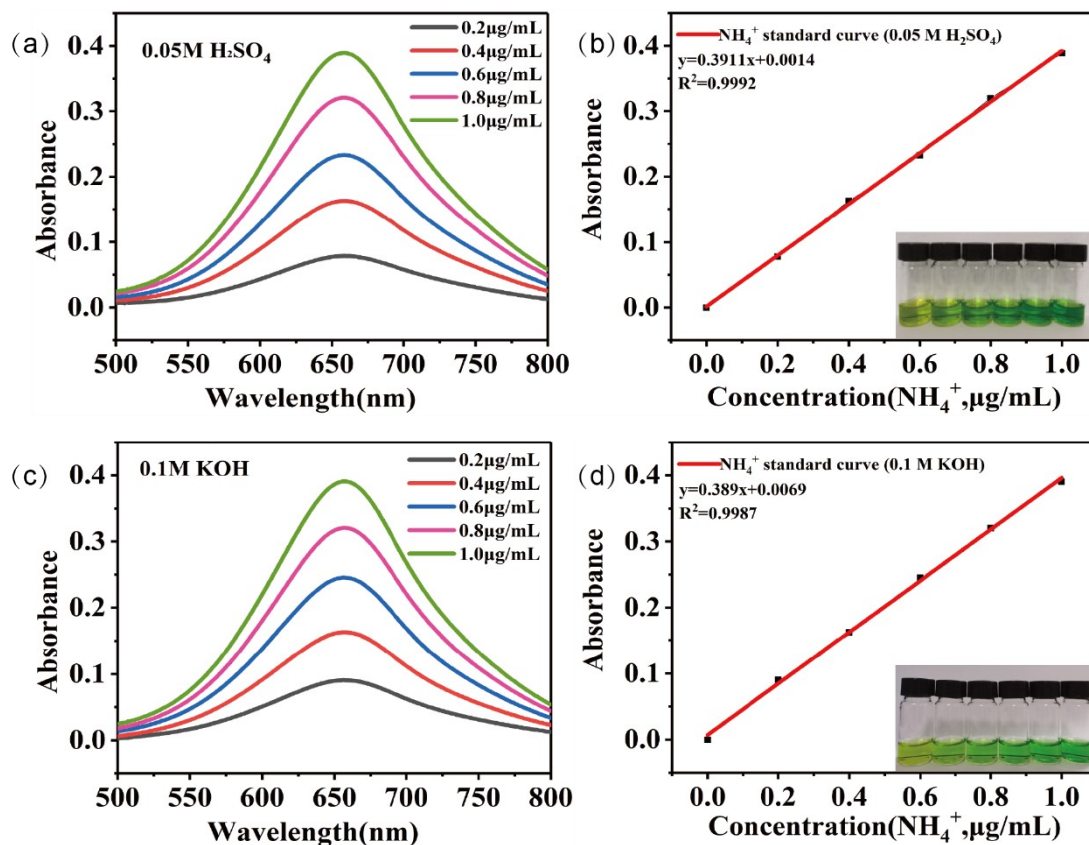
Fig.S10. (a) UV-vis absorption spectra of Indophenol assays with NH$_3$ in 0.05 M H$_2$SO$_4$ after incubated for 2h under ambient conditions. (b) Calibration curve used for calculation of NH$_3$ concentration. (c) UV-vis absorption spectra of Indophenol assays with NH$_3$ in 0.1 M KOH after incubated for 2h under ambient conditions. (d) Calibration curve used for calculation of NH$_3$ concentration.
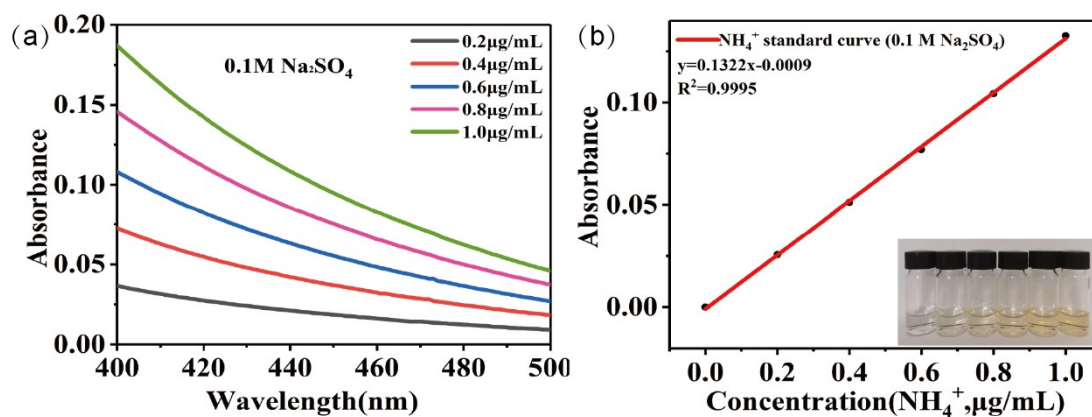
Fig.S11. (a) UV-vis absorption spectra of Nessler reagent assays with NH_3 in 0.1 M Na_2SO_4 after incubated for 2h under ambient conditions. (b) Calibration curve used for calculation of NH_3 concentration.

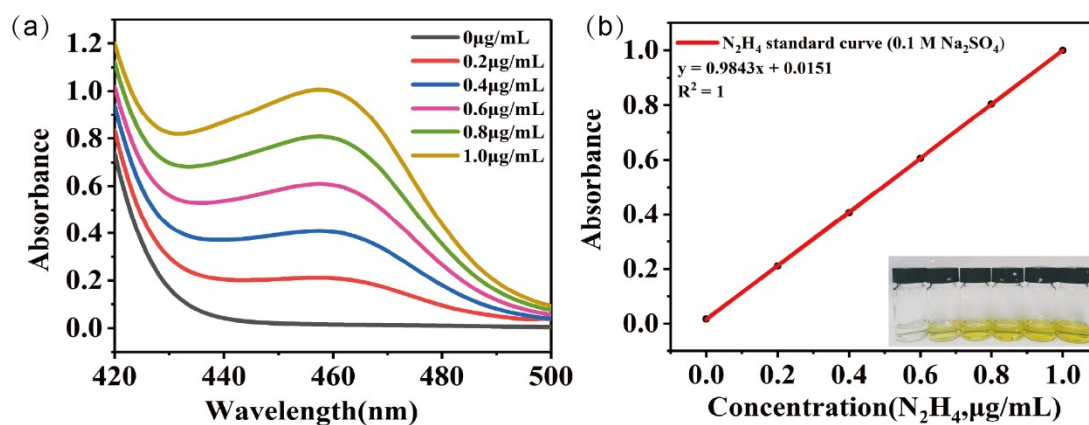Fig.S12: (a) UV-vis absorption spectra of various N_2H_4 concentrations stained with $C_9H_{11}NO$ indicator after incubated for 15 min under ambient conditions. (b) Calibration curve used for calculation of N_2H_4 concentration.

Table.S1. Comparison of the NRR electrocatalytic performance of LNO and other previously reported NRR electrocatalysts.

Catalyst	Electrolyte	NH$_3$ yield rate $\mu g\ mg_{cat}^{-1}\ h^{-1}$	FE (%)	Ref.
LiNb$_3$O$_8$	**0.1M Na$_2$SO$_4$**	**7.85**	**82.83**	**Our work**
Ru-ZIF-8	0.1M KOH	16.68	14.23	[1]
Pd	0.1M PBS	4.5	8.20	[2]
Au/Ni	0.05M H$_2$SO$_4$	7.4	67.8	[3]
Fe$_{sa}$-N-C	0.1M KOH	7.48	56.55	[4]
C18@Fe$_3$P	0.1M Na$_2$SO$_4$	1.80×10^{-10}mol·s^{-1}·cm^{-2}	11.22	[5]
MoS$_2$ NDs/rGO	0.1M Na$_2$SO$_4$	16.41	27.93	[6]
FeMo@NC	1.0M KOH	14.95	41.70	[7]
Ti$_3$C$_2$T$_x$ MXene	0.05M H$_2$SO$_4$	21.9	25.44	[8]
Co-N/S-N	0.05M Na$_2$SO$_4$	15.7	25.90	[9]
NiO/G	0.1M Na$_2$SO$_4$	18.6	7.8	[10]
CN/N	0.1M HCl	2.9	62.1	[11]
BiVO$_4$	0.2M Na$_2$SO$_4$	8.6	10.40	[12]

Reference:

1. Z. Zhang, K. Yao, L. Cong, Z. Yu, L. Qu and W. Huang, *Catalysis Science & Technology*, 2020, **10**, 1336-1342.

2. J. Wang, L. Yu, L. Hu, G. Chen, H. Xin and X. Feng, *Nat Commun*, 2018, **9**, 1795.

3. Z.-H. Xue, S.-N. Zhang, Y.-X. Lin, H. Su, G.-Y. Zhai, J.-T. Han, Q.-Y. Yu, X.-H. Li, M. Antonietti and J.-S. Chen, *Journal of the American Chemical Society*, 2019, **141**, 14976-14980.

4. M. Wang, S. Liu, T. Qian, J. Liul, J. Zhou, H. Ji, J. Xiong, J. Zhong and C. Yan, *Nature Communications*, 2019, **10**, 1-8.

5. T. Xu, J. Liang, Y. Wang, S. Li, Z. Du, T. Li, Q. Liu, Y. Luo, F. Zhang, X. Shi, B. Tang, Q. Kong, A. M. Asiri, C. Yang, D. Ma and X. Sun, *Nano Research*, 2021, DOI: 10.1007/s12274-021-3592-8.

6. Y. Liu, W. Wang, S. Zhang, W. Li, G. Wang, Y. Zhang, M. Han and H. Zhang, *Acs Sustainable Chemistry & Engineering*, 2020, **8**, 2320-2326.

7. Y. Li, Q. Zhang, C. Li, H.-N. Fan, W.-B. Luo, H.-K. Liu and S.-X. Dou, *Journal of Materials Chemistry A*, 2019, **7**, 22242-22247.

8. Y. Guo, T. Wang, Q. Yang, X. Li, H. Li, Y. Wang, T. Jiao, Z. Huang, B. Dong, W. Zhang, J. Fan and C. Zhi, *Acs Nano*, 2020, **14**, 9089-9097.

9. P. Chen, N. Zhang, S. Wang, T. Zhou, Y. Tong, C. Ao, W. Yan, L. Zhang, W. Chu, C. Wu and Y. Xie, *Proceedings of the National Academy of Sciences of the United States of America*, 2019, **116**, 6635-6640.

10. K. Chu, Y.-p. Liu, J. Wang and H. Zhang, *ACS Applied Energy Materials*, 2019, **2**, 2288-2295.

11. G. Peng, J. Wu, M. Wang, J. Niklas, H. Zhou and C. Liu, *Nano Letters*, 2020, **20**, 2879-2885.

12. J.-X. Yao, D. Boo, Q. Zhang, M.-M. Shi, Y. Wang, R. Gao, J.-M. Yan and Q. Jiang, *Small Methods*, 2019, **3**, 1800333.